RESEARCH ARTICLE | SEPTEMBER 14 2018

Predictive modeling of misfit dislocation induced strain relaxation effect on self-rolling of strain-engineered nanomembranes

Cheng Chen; Pengfei Song; Fanchao Meng; Pengfei Ou; Xinyu Liu; Jun Song

Appl. Phys. Lett. 113, 112104 (2018)
https://doi.org/10.1063/1.5046314

Predictive modeling of misfit dislocation induced strain relaxation effect on self-rolling of strain-engineered nanomembranes

Cheng Chen,[1] Pengfei Song,[2,3] Fanchao Meng,[1] Pengfei Ou,[1] Xinyu Liu,[3] and Jun Song[1,a)]
[1]*Department of Materials Engineering, McGill University, Montréal, Québec H3A0C5, Canada*
[2]*Department of Mechanical Engineering, McGill University, Montréal, Québec H3A0C3, Canada*
[3]*Department of Mechanical and Industrial Engineering, University of Toronto, Toronto, Ontario M5S3G8, Canada*

(Received 26 June 2018; accepted 29 August 2018; published online 14 September 2018)

Combining atomistic simulations and continuum modeling, the effects of misfit dislocations on strain relaxation and subsequently self-rolling of strain-engineered nanomembranes have been investigated. Two representative material systems including ($GaN/In_{0.5}Ga_{0.5}N$) of wurtzite lattice and II–VI materials ($CdTe/CdTe_{0.5}S_{0.5}$) of zinc-blend lattice were considered. The atomistic characteristics of dislocation and the resulting lattice distorting were first determined by generalized-stacking-fault energy profile and disregistry function obtained through Peierls-Nabarro model. Those properties were then used to calculate the accurate mismatch strain of those nanomembranes with the presence of dislocations, and as inputs into von-Karman shell theory to quantitatively evaluate the effects on self-rolling curvature and anisotropy. The theoretical results were further confirmed by atomistic simulations of different crystal geometries and dislocation configurations. Our results provide essential theoretical insights towards prediction and design of rollup configurations for strain-engineered nanomembranes containing crystalline defects. *Published by AIP Publishing.* https://doi.org/10.1063/1.5046314

Offering unique mechanical flexibility and geometrical variabilities along with excellent machinability, the rolled-up nanotechnology involving nanomembranes that consist of two or more strained layers has emerged as the focus of interest for numerous advanced applications including drug delivery,[1,2] optical microcavity,[3–6] optoelectronics,[7–11] artificial biomimetic structures,[12–20] micro/nanoscale motors,[21–23] and on-chip energy storage integrated microdevices,[24–26] among others. The essential functional principle for the rolled-up nanotechnology relies on engineered strain gradient embedded in bi- or multilayer nanomembranes, which drives nanomembranes to self rolled-up into tubular geometries with tunable diameters once detached and relaxed from their host substrates.[27] For semiconductor nanomembranes, engineering of the strain gradient therein can be achieved through adjusting the composition dependent lattice mismatch of the strained layers utilizing heteroepitaxial deposition methods involving, e.g., molecular beam epitaxy (MBE) and metalorganic chemical vapour deposition (MOCVD).[28–30] Both methods not only can precisely manipulate the composition and thickness of nanomembranes at the monolayer scale to enable strain gradient tuning, but also are applicable to a wide range of nanomembrane materials, such as Group IV (e.g., Si/Ge),[31–33] III–V (e.g., InGaN/GaN),[6,29,30,34–37] and II–VI (e.g., CdS/CdSe) materials.[38,39]

In contrast to the existing capability and flexibility in engineer the strain, accurate determination of the mismatch strain, on the other hand, can be challenging, particularly in cases of large strains[40] and film thickness,[35,37,41,42] as the mismatch strain could be partially relaxed via the nucleation of misfit dislocations at the interface. Consequently, the strain gradient cannot be well evaluated by considering only lattice mismatch. Moreover, in certain cases, especially for the epitaxial growth of highly mismatched materials, periodic interfacial misfit dislocations are intentionally introduced to effectively alleviate the mismatch strain and reduce the density of vertically propagating threading dislocations that are highly detrimental to device performance.[43,44] However, despite the importance in affecting the strain in the nanomembrane, there has been limited work to investigate the dislocation induced strain relaxation and its subsequent effect on the self-rolling behaviors of strain engineered nanomembranes. This deficit prevents the precise prediction and manipulation of the geometry of rolled-up nanomembranes where dislocations exist.

In this paper, we present a systematic study, aiming to address the afore-mentioned deficit in the understanding of the role of misfit dislocations on self-rolling of strain-engineered nanomembranes, combining atomistic simulations and continuum modeling. Two bilayer material models, the $GaN/In_{0.5}Ga_{0.5}N$ (III–V materials) of wurtzite lattice and $CdTe/CdTe_{0.5}S_{0.5}$ (II–VI materials) of zinc-blend lattice, were chosen as representatives of nanomembrane systems in the present study. Stable misfit dislocation configurations at the interface were constructed and examined using atomistic simulations. The effects of strain relaxation and strain distribution induced by misfit dislocations were quantitatively determined by the disregistry functions obtained through the Peierls-Nabarro (PN) model with generalized-stacking-fault energy (GSFE) profiles of those dislocations as inputs. The effects of misfit dislocations on self-rolling curvatures of strain-engineered nanomembranes were then further evaluated employing the von-Karman shell theory combined with disregistry functions, validated by atomistic simulations. Our study provides a theoretical approach that explicitly accounts for the misfit dislocations induced strain

a)Author to whom correspondence should be addressed: jun.song2@mcgill.ca, Tel.: +1 (514) 398-4592, Fax: +1 (514) 398-4492

relaxation for predictive engineering of self-rolling of strained nanomembranes.

Atomistic simulations of dislocation effects on self-rolling were performed in the framework of classical molecular dynamics (MD) implemented in the LAMMPS package employing the Stillinger-Weber potentials[45–50] for the ternary systems of Cd-S-Te[51] and In-Ga-N.[52] Typical misfit dislocations identified in the heterostructures of CdTe/$CdTe_{0.5}S_{0.5}$ and GaN/$In_{0.5}Ga_{0.5}N$, i.e., $\vec{b}_1 = 1/2[011]$ of the $(001)[011]$ slip system and $\vec{b}_2 = 1/3[11\bar{2}0]$ of the $(1\bar{1}00)[11\bar{2}0]$ slip system respectively, were considered. The atomic configurations of interfaces in those heterostructures and core structures of the corresponding dislocations considered are illustrated in Figs. 1(a)–1(d).

Large-scale MD simulations were then performed to examine the self-rolling of strain-engineered nanomembranes with different misfit dislocations densities at the interface, with the model schematically illustrated in Figs. 1(b) and 1(d). (The detailed description of the simulation model and settings, and the rolling process are presented in the supplementary material.)

The lattice distortion induced by the interface misfit dislocations was analyzed in terms of the disregistry function, which describes the relative displacement between two half crystals at the interface. The disregistry function was obtained through Peierls-Nabarro (PN) model[53–56] together with the GSFE of the dislocation as input (see the calculated GSFE curves in supplementary material). Afterwards, based on those GSFE curves, the disregistry function $u(x)$ (with x being the coordinate normalized by the magnitude of Burgers vector) can be deduced by considering the balance between the stress induced by the dislocation and the periodic lattice restoring stress $-\frac{\partial \gamma_{GSFE}(u(x))}{\partial u(x)}$ that represents the lattice resistance of a crystal to the distortion associated with the dislocation core

$$K\int_{-\infty}^{\infty}\frac{(du(x)/dx)_{x=x'}dx'}{x-x'} = -\frac{\partial \gamma_{GSFE}(u(x))}{\partial u(x)}, \tag{1}$$

where γ_{GSFE} is the GSFE energy, K is a constant, $\mu/(4\pi)$ being for a screw dislocation and $\mu/[4\pi(1-\nu)]$ for an edge dislocation, μ and ν are the shear modulus along the slip plane of dislocation and Poisson's ratio, respectively. Because the misfit dislocations are located at the interface of nanomembranes, μ and ν are taken to be the average value of the system, namely, 38 GPa and 0.33 for CdTe/$CdTe_{0.5}S_{0.5}$, while 108 GPa and 0.25 for GaN/$In_{0.5}Ga_{0.5}N$. The disregistry function $u(x)$ and the associated disregistry density $\rho(x) = \frac{du(x)}{dx}$ are then are then obtained as depicted in Figs. 2(b) and 2(d), based on the method of trial fitting functions,[57,58] where it is assumed that

$$u(x) = \frac{b}{\pi}\sum_{i=1}^{n}\alpha_i \arctan\frac{x-x_i}{c_i} + \frac{b}{2}, \quad \text{where} \quad \sum_{i}^{n}\alpha_i = 1. \tag{2}$$

In the above, the single-arctan approximation ($n = 1$ and $x_1 = 0$) has been found to provide an accurate estimation for the disregistry function. Thus, Eq. (2) simplifies to

$$u(x) = \frac{b}{\pi}\arctan\frac{x}{c_1} + \frac{b}{2}, \tag{3}$$

where the parameter c_1 is calculated to be 0.525 and 0.252 for the systems of CdTe/$CdTe_{0.5}S_{0.5}$ and GaN/$In_{0.5}Ga_{0.5}N$, respectively. Consequently the distortion induced by the misfit dislocation can be expressed as a nonlinear, continuous function of the coordinate x along the Burger's vector direction, reaching the maximum value at the dislocation core region. Therefore, the inelastic strain ε^{in} of the system that includes the mismatch strain at the heterogeneous interface

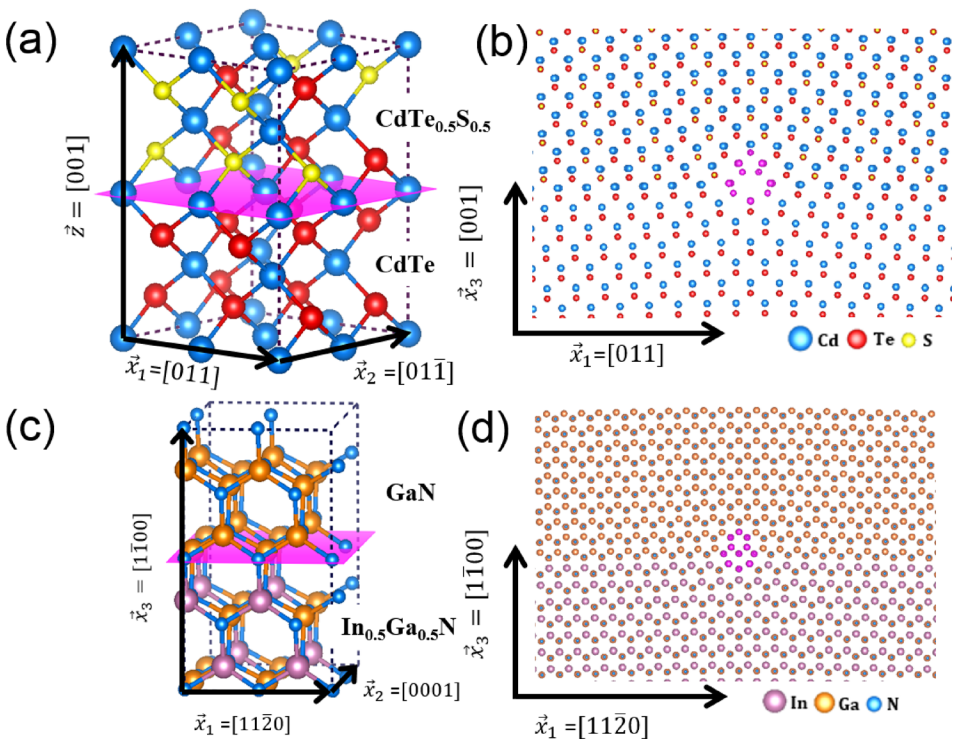

FIG. 1. Three dimensional schematic illustrations of the (a) zinc blend CdS/$CdTe_{0.5}S_{0.5}$ and (c) wurtzite GaN/$In_{0.5}Ga_{0.5}N$ bilayer systems, where the shaded plane indicated the interface. (b) The 5 and 7-ring core configuration for the $1/2[011](001)$ edge dislocation on the mismatched interface of CdS/$CdTe_{0.5}S_{0.5}$ (projection view along $[01\bar{1}]$ direction) and (d) the 8-ring core for the $1/3[11\bar{2}0]$ edge dislocation residing in the mismatched interface of GaN/$In_{0.5}Ga_{0.5}N$ (projection view along [0001] direction). Cd, Te, and S atoms are colored blue, red and yellow, respectively. N atoms are indicated by small blue spheres, while In and Ga atoms are represented by purple and golden spheres.

and distortion induced by misfit dislocations can be determined through the principle of superposition, as shown in the following equation:

$$\varepsilon^{in} = \varepsilon_0 + \sum_{i=1}^{n} \frac{\partial u\left(x + hx_i^d\right)}{\partial x}, \tag{4}$$

where ε_0 and n indicate the original mismatch strain and number of misfit dislocations, respectively, and x_i^d represents the distance between two closed dislocations.

Combining the von-Karman shell theory[59] and disregistry functions of dislocations obtained, the dislocation effect on rolled-up curvatures of nanomembranes can then be predicted numerically, as elaborated below. Figure 2(a) depicts a typical precursor geometry of a strained nanomembrane with embedded misfit dislocations embedded, where the corresponding atomistic details of the rolled-up structures are further illustrated in Figs. 2(b) and 2(c) (Multimedia view). Assuming a plane-stress formulation, the total potential energy H of this system can be expressed as a function of the mechanical and geometrical properties of nanomembranes

$$H = \int_0^{L_{x_1}} \int_0^{L_{x_2}} \left(\int_{-L_{x_3}/2}^{L_{x_3}/2-h_t} Q_{ij}^b \varepsilon_i^b \varepsilon_j^b dx_3 + \int_{L_{x_3}/2-h_t}^{L_{x_3}/2} Q_{ij}^t \varepsilon_i^t \varepsilon_j^t dx_3 \right) dx_2 dx_1, \tag{5}$$

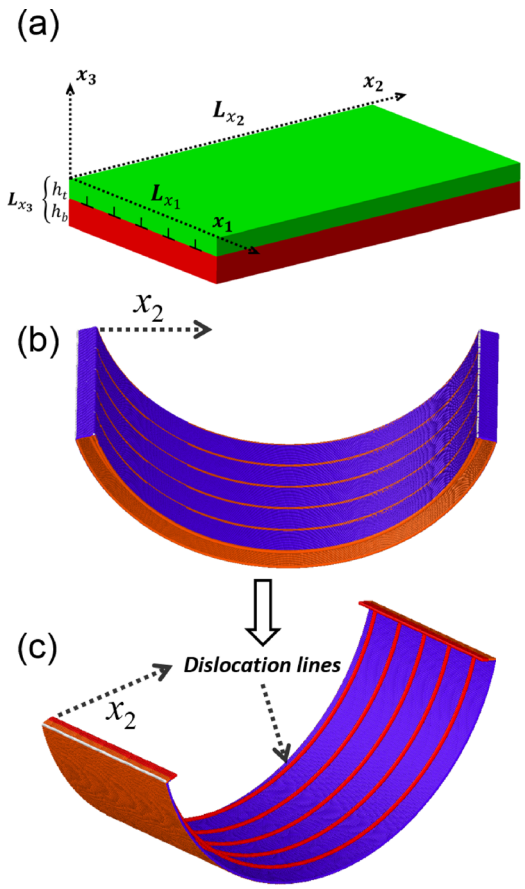

FIG. 2. (a) Schematic illustration of the initial geometry of a nanomembrane with misfit dislocations at the interface of strained bilayers. A representative resultant rolled-up structure is illustrated in (b), with (c) showing the section profile that highlights the dislocation lines, which are colored red. Multimedia view: https://doi.org/10.1063/1.5046314.1

where L_{x_1}, L_{x_2}, and L_{x_3} are the lengths of the nanomembrane in the x_1, x_2, and x_3 directions, respectively, with L_{x_3} being effectively the total thickness of the nanomembrane. (h_t, h_b) and (Q_{ij}^t, Q_{ij}^b) ($i, j = 1, 2, 6$) denote the individual thicknesses and transformed reduced elastic stiffnesses[52] of top and bottom layers, respectively. Note that (Q_{ij}^t, Q_{ij}^b) effectively incorporates the dependence of elastic constants on the crystal orientation (see supplementary material). For the CdTe/$CdTe_{0.5}S_{0.5}$ and GaN/$In_{0.5}Ga_{0.5}N$ systems considered, the transformed reduced elastic stiffnesses (Q_{ij}^t, Q_{ij}^b) of nanomembranes used in the numerical calculations are obtained and enlisted in Table S1 (see supplementary material). Meanwhile, $\left(\varepsilon_i^b, \varepsilon_j^b\right)$ and $\left(\varepsilon_i^t, \varepsilon_j^t\right)$ define the in-plane elastic strains in the bottom and top layer with $i, j = 1, 2, 6$ as per convention,[52] given by

$$\varepsilon_1^b = \varepsilon_1^m + x_3\kappa_1, \quad \varepsilon_2^b = \varepsilon_2^m + x_3\kappa_2, \tag{6}$$

$$\varepsilon_1^t = \varepsilon_1^m + x_3\kappa_1 - \varepsilon_1^{in}, \quad \varepsilon_2^t = \varepsilon_2^m + x_3\kappa_2 - \varepsilon_2^{in}, \tag{7}$$

with (ε_1^m, ε_2^m) and (κ_1, κ_2) being the mid-plane strains and curvatures, respectively, defined as

$$\varepsilon_1^m = \frac{\partial u_1}{\partial x_1} + \frac{1}{2}\left(\frac{\partial u_3}{\partial x_1}\right)^2, \quad \varepsilon_2^m = \frac{\partial u_2}{\partial x_2} + \frac{1}{2}\left(\frac{\partial u_3}{\partial x_1}\right)^2, \tag{8}$$

$$\kappa_1 = \frac{\partial^2 u_3}{\partial x_1^2}, \quad \kappa_2 = \frac{\partial^2 u_3}{\partial x_2^2}, \tag{9}$$

where u_i ($i = 1, 2, 3$) are the mid-plane displacements of the nanomembranes in the x_1, x_2, and x_3 directions. Here, for the numerical purpose, the mid-plane displacements can be approximated using polynomials[60,61]

$$u_1 = \sum_{i,j=0}^{3} c_{ij} x_1^i x_2^j, \quad u_2 = \sum_{i,j=0}^{3} d_{ij} x_1^i x_2^j, \tag{10}$$

where the c_{ij} and d_{ij} are to-be-determined coefficients. In our calculations, an approximated displacement field is assumed for u_3 based on the Ritz method[62,63] as

$$u_3 = \frac{1}{2}\left(ax_1^2 + bx_2^2\right), \tag{11}$$

where a and b are parameters to be determined.

The coefficients and curvatures can then be obtained by minimizing the potential energy H. We can then start to examine the self-rolling behaviors and preference of rolling directions of nanomembranes containing dislocations. Figure 3 shows the equilibrium strain energies (normalized with respect to that of the corresponding flat nanomembrane) of CdTe/$CdTe_{0.5}S_{0.5}$ and GaN/$In_{0.5}Ga_{0.5}N$ systems for the two rolled-up states along x_1 and x_2 directions, as functions of the misfit dislocation density ρ_d, defined as the dislocation number per unit length along Burger's vector direction (i.e., x_1). As seen in Fig. 3, the presence of dislocations leads to smaller strain energy for rolling along the x_2 direction for both material systems, with the difference in strain energy between the two rolling modes (i.e., along x_1 and along x_2) increasing as ρ_d increases. This suggests that the x_2 direction be the preferred rolling direction in the presence of misfit

dislocations. This can be explained by the strain relaxation along the x_1 direction (the Burger's vector direction) induced by misfit dislocations, resulting in the reduced bend force. It is also worth noting that the afore-mentioned rolling preference does not change as the layer thicknesses (h_t and h_b) vary, though increasing the h_t/h_b ratio will decrease the equilibrium strain energies for both rolling along the x_1 and x_2 directions. Therefore, below we only discuss rolling along the x_2 direction and examine the evolution of the curvature κ_2 as the misfit dislocation density and layer thickness vary, which are compared with the one obtained from MD simulations (a separate discussion of rolling along the x_1 direction is included in supplementary material). The rolled-up diameter is measured at the mid-plane of the rolled-up geometry through fitting and averaging the trajectories of high-energy atoms on the bottom and top surfaces. The MD simulated evolution of rolled-up diameter as a function of the dislocation density with varied thickness of top layer is presented in Fig. 4, in comparison with the model predictions obtained from Eqs. (8) to (11). It is observed from MD simulation results that there is the rolling diameter increases monotonically as the misfit dislocation or the top layer thickness increases, which is accurately predicted by our theoretical model. The results in Fig. 4 confirm the accuracy of our model in accounting for the dislocation effect and subsequently predicting the rolling behaviors of nanomembranes.

This work presents a systematic work combining atomistic simulations and continuum modeling to study the effect of misfit dislocations on self-rolling of strain-engineered nanomembranes, using GaN/$In_{0.5}Ga_{0.5}N$ and CdTe/$CdTe_{0.5}S_{0.5}$ as representative nanomembrane systems. The generalized stacking fault energy (GSFE) curves corresponding to typical mismatch dislocations in those material systems were calculated from atomistic simulations as inputs for the Peierls-Nabarro (PN) model to obtain the disregistry functions of dislocations and thus determine the lattice elastic distortion associated with dislocations. A theoretical model was then formulated employing von-Karman shell theory with the disregistry functions incorporated. It was demonstrated that the presence of misfit dislocations can modulate the competition between different rolling directions to cause anisotropic rolling of strain-engineered nanomembranes. The developed model was shown to accurately predict the rolled-up curvature of strained nanomembranes with different crystal symmetries and misfit dislocation configurations, validated by atomistic simulations. The model provides a valuable predictive tool for quantitative assessment of the role of mismatch defects and precise design of the rolled-up structures from pre-defined geometries of strain-engineered nanomembranes, particularly for situations involving large mismatch strain and layer thickness. It also provides essential theoretical support for the application of self-rolling technology to high lattice-mismatch ternary semiconductor systems, such as $In_xGa_{1-x}Sb$ alloys directly grown on GaAs substrates, and defect engineering which may serve as a potential means towards predictive curve tuning in self-rolling nanomembranes through controlled manipulation of dislocations.

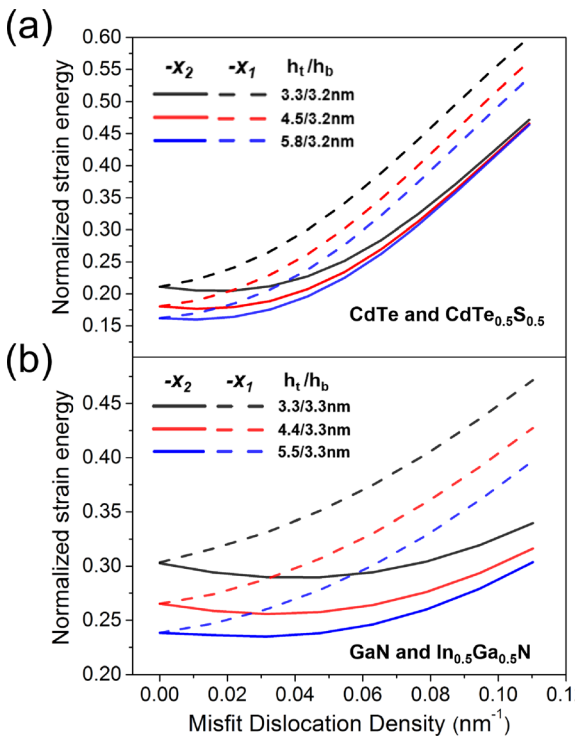

FIG. 3. Strain energies of rollup structures of the (a) CdTe/$CdTe_{0.5}S_{0.5}$ and (b) GaN/$In_{0.5}Ga_{0.5}N$ systems (normalized with respect to the strain energy of the corresponding flat nanomembrane) are plotted against misfit dislocation densities for rolling up along $-x_1$ and $-x_2$ directions with varied thickness ratio of top and bottom layers.

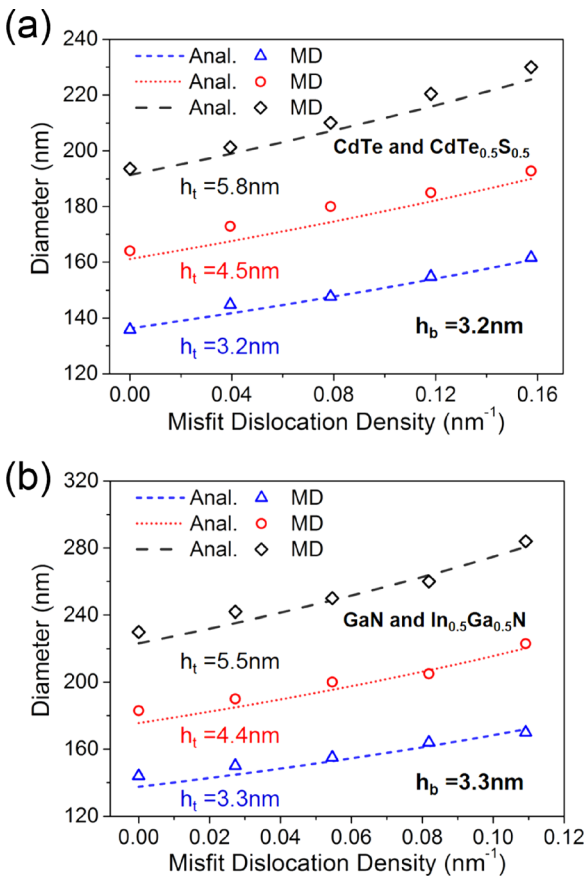

FIG. 4. The predicted and MD simulated rolling diameter as a function of the misfit dislocation density with varied thickness of top layer for (a) CdTe/$CdTe_{0.5}S_{0.5}$ and (b) GaN/$In_{0.5}Ga_{0.5}N$, respectively, in comparison with the model predictions obtained from Eqs. (8) to (11).

See supplementary material for details on MD simulations of self-rolling process and characteristics of misfit dislocations.

We greatly thank the financial support from McGill Engineering Doctoral Award, China Scholarship Council, National Sciences and Engineering Research Council (NSERC) Discovery grant (Grant No. RGPIN-2017-05187), and NSERC Strategic grant (Grant No. STPGP 494012-16). We also acknowledge Supercomputer Consortium Laval UQAM McGill and Eastern Quebec for providing computing power.

[1]R. Arayanarakool, A. K. Meyer, L. Helbig, S. Sanchez, and O. G. Schmidt, Lab Chip **15**, 2981 (2015).
[2]R. Fernandes and D. H. Gracias, Adv. Drug Delivery Rev. **64**, 1579 (2012).
[3]G. S. Huang and Y. F. Mei, J. Mater. Chem. C **5**, 2758 (2017).
[4]J. Wang, T. R. Zhan, G. S. Huang, P. K. Chu, and Y. F. Mei, Laser Photonics Rev. **8**, 521 (2014).
[5]X. L. Li, Adv. Opt. Photonics **3**, 366 (2011).
[6]T. Kipp, H. Welsch, C. Strelow, C. Heyn, and D. Heitmann, Phys. Rev. Lett. **96**, 077403 (2006).
[7]S. M. Harazim, V. A. B. Quinones, S. Kiravittaya, S. Sanchez, and O. G. Schmidt, Lab Chip **12**, 2649 (2012).
[8]A. Bernardi, S. Kiravittaya, A. Rastelli, R. Songmuang, D. J. Thurmer, M. Benyoucef, and O. G. Schmidt, Appl. Phys. Lett. **93**, 094106 (2008).
[9]S. M. Harazim, W. Xi, C. K. Schmidt, S. Sanchez, and O. G. Schmidt, J. Mater. Chem. **22**, 2878 (2012).
[10]Q. L. Guo, Z. F. Di, M. G. Lagally, and Y. F. Mei, Mater. Sci. Eng. Rep. **128**, 1 (2018).
[11]W. Huang, J. Zhou, P. J. Froeter, K. Walsh, S. Liu, M. D. Kraman, M. Li, J. A. Michaels, D. J. Sievers, S. Gong, and X. Li, Nat. Electronics **1**, 305 (2018).
[12]K. U. Jeong, J. H. Jang, D. Y. Kim, C. Nah, J. H. Lee, M. H. Lee, H. J. Sun, C. L. Wang, S. Z. D. Cheng, and E. L. Thomas, J. Mater. Chem. **21**, 6824 (2011).
[13]L. Ionov, Adv. Funct. Mater. **23**, 4555 (2013).
[14]L. Persano, A. Camposeo, and D. Pisignano, J. Mater. Chem. C **1**, 7663 (2013).
[15]R. Kempaiah and Z. H. Nie, J. Mater. Chem. B **2**, 2357 (2014).
[16]M. Podgorski, D. P. Nair, S. Chatani, G. Berg, and C. N. Bowman, ACS Appl. Mater. Interfaces **6**, 6111 (2014).
[17]A. R. Studart, Angew. Chem., Int. Ed. **54**, 3400 (2015).
[18]F. M. Wisser, B. Schumm, G. Mondin, J. Grothe, and S. Kaskel, J. Mater. Chem. C **3**, 2717 (2015).
[19]A. S. Gladman, E. A. Matsumoto, R. G. Nuzzo, L. Mahadevan, and J. A. Lewis, Nat. Mater. **15**, 413 (2016).
[20]Z. Tian, W. Huang, B. Xu, X. Li, and Y. Mei, Nano Lett. **18**, 3688 (2018).
[21]H. Wang and M. Pumera, Chem. Rev. **115**, 8704 (2015).
[22]J. X. Li, J. Zhang, W. Gao, G. S. Huang, Z. F. Di, R. Liu, J. Wang, and Y. F. Mei, Adv. Mater. **25**, 3715 (2013).
[23]A. A. Solovev, Y. F. Mei, E. B. Urena, G. S. Huang, and O. G. Schmidt, Small **5**, 1688 (2009).
[24]X. F. Wang, Y. Chen, O. G. Schmidt, and C. L. Yan, Chem. Soc. Rev. **45**, 1308 (2016).
[25]X. H. Liu, J. Zhang, W. P. Si, L. X. Xi, B. Eichler, C. L. Yan, and O. G. Schmidt, ACS Nano **9**, 1198 (2015).
[26]L. Zhang, J. W. Deng, L. F. Liu, W. P. Si, S. Oswald, L. X. Xi, M. Kundu, G. Z. Ma, T. Gemming, S. Baunack, F. Ding, C. L. Yan, and O. G. Schmidt, Adv. Mater. **26**, 4527 (2014).
[27]Z. Chen, G. S. Huang, I. Trase, X. M. Han, and Y. F. Mei, Phys. Rev. Appl. **5**, 017001 (2016).
[28]I. S. Chun, A. Challa, B. Derickson, K. J. Hsia, and X. L. Li, Nano Lett. **10**, 3927 (2010).
[29]I. S. Chun, V. B. Verma, V. C. Elarde, S. W. Kim, J. M. Zuo, J. J. Coleman, and X. Li, J. Crystal Growth **310**, 2353 (2008).
[30]C. Deneke, C. Muller, N. Y. Jin-Phillipp, and O. G. Schmidt, Semicond. Sci. Technol. **17**, 1278 (2002).
[31]F. Cavallo and M. G. Lagally, Soft Matter **6**, 439 (2010).
[32]F. Cavallo, R. Songmuang, and O. G. Schmidt, Appl. Phys. Lett. **93**, 143113 (2008).
[33]F. Cavallo, R. Songmuang, C. Ulrich, and O. G. Schmidt, Appl. Phys. Lett. **90**, 193120 (2007).
[34]N. Y. Jin-Phillipp, J. Thomas, M. Kelsch, C. Deneke, R. Songmuang, and O. G. Schmidt, Appl. Phys. Lett. **88**, 033113 (2006).
[35]F. Li and Z. T. Mi, Opt. Express **17**, 19933 (2009).
[36]Z. B. Tian, V. Veerasubramanian, P. Bianucci, S. Mukherjee, Z. T. Mi, A. G. Kirk, and D. V. Plant, Opt. Express **19**, 12164 (2011).
[37]Z. B. Tian, F. Li, Z. T. Mi, and D. V. Plant, IEEE Photonics Technol. Lett. **22**, 311 (2010).
[38]J. Q. Hu, Y. Bando, J. H. Zhan, M. Y. Liao, D. Golberg, X. L. Yuan, and T. Sekiguchi, Appl. Phys. Lett. **87**, 113107 (2005).
[39]R. B. Vasiliev, E. P. Lazareva, D. A. Karlova, A. V. Garshev, Y. Z. Yao, T. Kuroda, A. M. Gaskov, and K. Sakoda, Chem. Mater. **30**, 1710 (2018).
[40]Y. F. Mei, D. J. Thurmer, C. Deneke, S. Kiravittaya, Y. F. Chen, A. Dadgar, F. Bertram, B. Bastek, A. Krost, J. Christen, T. Reindl, M. Stoffel, E. Coric, and O. G. Schmidt, ACS Nano **3**, 1663 (2009).
[41]X. Li and W. Huang, Google Patent 8,941,460 (2014).
[42]J. Wang, E. M. Song, C. L. Yang, L. R. Zheng, and Y. F. Mei, Thin Solid Films **627**, 77 (2017).
[43]S. H. Huang, G. Balakrishnan, M. Mehta, A. Khoshakhlagh, L. R. Dawson, D. L. Huffaker, and P. Li, Appl. Phys. Lett. **90**, 161902 (2007).
[44]S. H. Huang, G. Balakrishnan, A. Khoshakhlagh, A. Jallipalli, L. R. Dawson, and D. L. Huffaker, Appl. Phys. Lett. **88**, 131911 (2006).
[45]F. H. Stillinger and T. A. Weber, Phys. Rev. B **31**, 5262 (1985).
[46]S. Plimpton, J. Comput. Phys. **117**, 1 (1995).
[47]X. W. Zhou, M. E. Foster, F. B. van Swol, J. E. Martin, and B. M. Wong, J. Phys. Chem. C **118**, 20661 (2014).
[48]J. Gruber, X. W. Zhou, R. E. Jones, S. R. Lee, and G. J. Tucker, J. Appl. Phys. **121**, 195301 (2017).
[49]X. W. Zhou, J. J. Chavez, S. Almeida, and D. Zubia, J. Appl. Phys. **120**, 045304 (2016).
[50]X. W. Zhou, D. K. Ward, J. A. Zimmerman, J. L. Cruz-Campa, D. Zubia, J. E. Martin, and F. van Swol, J. Mech. Phys. Solids **91**, 265 (2016).
[51]X. W. Zhou, D. K. Ward, J. E. Martin, F. B. van Swol, J. L. Cruz-Campa, and D. Zubia, Phys. Rev. B **88**, 085309 (2013).
[52]X. W. Zhou, R. E. Jones, and J. Gruber, Comput. Mater. Sci. **128**, 331 (2017).
[53]C. Chen, F. C. Meng, and J. Song, J. Appl. Phys. **119**, 064302 (2016).
[54]C. Chen, F. C. Meng, and J. Song, J. Appl. Phys. **117**, 194301 (2015).
[55]F. Nabarro, Proc. Phys. Soc. **59**, 256 (1947).
[56]R. Peierls, Proc. Phys. Soc. **52**, 34 (1940).
[57]V. Bulatov and W. Cai, *Computer Simulations of Dislocations* (OUP Oxford, 2006).
[58]V. V. Bulatov and E. Kaxiras, Phys. Rev. Lett. **78**, 4221 (1997).
[59]S. Vidoli, Int. J. Solids Struct. **50**, 1241 (2013).
[60]C. Cheng, S. Pengfei, M. Fanchao, L. Xiao, L. Xinyu, and S. Jun, Nanotechnology **28**, 485302 (2017).
[61]C. Cheng, S. Pengfei, M. Fanchao, O. Pengfei, L. Xinyu, and S. Jun, Nanotechnology **29**, 345301 (2018).
[62]M. L. Dano and M. W. Hyer, Int. J. Solids Struct. **35**, 2101 (1998).
[63]M. W. Hyer, J. Compos. Mater. **15**, 296 (1981).